Progress in Reaction Kinetics and Mechanism

ARTICLE

Open Access

https://doi.org/10.48130/prkm-0026-0023

Progress in Reaction Kinetics and Mechanism **2026**, 51: e029

A non-classical pathway for selective *N*-functionalization in water: kinetic and mechanistic evidence beyond Schotten–Baumann reaction

Geun Ho Kim[1] and Jung Woon Yang[1,2*]

[1] *Department of Energy Science, Sungkyunkwan University, Suwon 16419, Republic of Korea*
[2] *Department of Energy, Sungkyunkwan University, Suwon 16419, Republic of Korea*
* Correspondence: jwyang@skku.edu (Yang JW)

Abstract

Efficient and selective amidation in water remains challenging because productive *N*-acylation competes with hydrolysis of the acylating agent. Although acyl fluorides exhibit greater hydrolytic stability than acyl chlorides, the mechanistic origins of their unusual reactivity and selectivity in water remain poorly understood. Combined kinetic, spectroscopic, and computational investigations reveal a previously unknown acyl-transfer pathway arising from the cooperative assembly of an acyl fluoride, a potassium ion (derived from K_2CO_3), and water, generating a water-solvated mimic of the 18-crown-6–K^+ complex that fundamentally alters acyl-transfer reactivity under aqueous conditions. This activation mode enables carbonate-mediated formation of a carbonic mixed anhydride, whose enhanced resistance to hydrolysis relative to the corresponding acyl halide decisively favors productive *N*-functionalization over competing hydrolysis. Under the optimized K_2CO_3-mediated conditions, the model amidation afforded the amide in > 99% yield within 1 h, with no detectable hydrolysis product (> 99:n.d.), whereas the classical biphasic Schotten–Baumann reaction using benzoyl chloride and KOH in CH_2Cl_2/H_2O afforded the corresponding amide in 76% yield with an amide-to-hydrolysis-product ratio of 96:4. The resulting mechanism enables highly selective amidation under fully aqueous conditions and reveals a previously unrecognized mode of aqueous acyl transfer. Beyond elucidating the origins of acyl fluoride reactivity in water, this work establishes a kinetic and mechanistic foundation for the rational design of sustainable acylation chemistry and reveals a non-classical acyl-transfer mechanism that transcends the inherent limitations of classical Schotten–Baumann methodology.

Keywords: Acyl fluoride, Carbonate-mediated acyl transfer, Aqueous amidation, Non-classical Schotten–Baumann reaction, Carbonic mixed anhydride

Citation: Kim GH, Yang JW. 2026. A non-classical pathway for selective *N*-functionalization in water: kinetic and mechanistic evidence beyond Schotten–Baumann reaction. *Progress in Reaction Kinetics and Mechanism* 51: e029 https://doi.org/10.48130/prkm-0026-0023

Introduction

Insights into reaction kinetics and mechanisms provide a foundation for understanding the molecular origins of chemical reactivity and for guiding the rational development of more efficient and selective synthetic transformations[1–3]. Such understanding is particularly important for reactions performed in aqueous media, where productive bond-forming processes often compete with solvent-induced decomposition pathways[4–6].

Amide bond formation is one of the most widely utilized transformations in organic synthesis and is indispensable for the preparation of pharmaceuticals, functional materials, and biologically active molecules[7–9]. Among the available synthetic methods, the Schotten–Baumann reaction remains a practical and widely adopted protocol, enabling the conversion of amines and acyl chlorides into amides under aqueous basic conditions[10,11]. Despite its practicality and widespread use, the reaction is constrained by an inherent incompatibility between the requirements of acid scavenging and acylating-agent stability[12–14]. Efficient amidation requires an aqueous basic phase to continuously neutralize the HCl generated during acylation and preserve amine nucleophilicity[12,13,15]. At the same time, highly reactive acyl chlorides readily undergo hydrolysis in water, leading to carboxylic acid formation and loss of reaction efficiency[16,17]. Consequently, successful Schotten–Baumann acylation depends on maintaining a delicate balance between productive amidation and competing hydrolysis.

To overcome the inherent incompatibility between acid scavenging and acyl chloride stability, Schotten–Baumann reactions are conventionally performed in biphasic aqueous–organic systems[10,18,19]. Although phase separation suppresses hydrolysis and preserves acylation efficiency, it does so through extensive reliance on organic solvents, including environmentally hazardous halogenated media such as CH_2Cl_2 and highly flammable ethers such as Et_2O, as well as on interfacial transport processes[18,20,21]. As a consequence, the sustainability of the transformation remains fundamentally tied to solvent-assisted hydrolysis control, motivating the search for acylation strategies capable of operating efficiently in water without the need for a separate organic phase[22–24].

Acyl fluorides have recently attracted considerable interest owing to their unique synthetic versatility, as they can serve as acyl ('RCO'), alkyl/aryl ('R'), and fluorine ('F') sources in a wide range of organic transformations[25–27]. In particular, they have emerged as highly attractive acylating agents because fluorine incorporation imparts unique electronic and physicochemical properties[28–30], giving rise to an exceptional combination of hydrolytic stability and acyl-transfer reactivity[26,31,32]. The synthetic utility of acyl fluorides in amide bond formation has been demonstrated in several studies. SuFEx-mediated amidation enables the *in situ* conversion of carboxylic acids into acyl fluorides for the synthesis of sterically hindered and electron-deficient amides[33], while PFP-mediated deoxyfluorination–amidation proceeds through *in situ*-generated acyl fluoride intermediates[34]. These approaches demonstrated the utility of acyl fluorides for amide synthesis but relied on their *in situ* generation and subsequent amidation in organic media. In contrast, the present

© The Author(s)

https://doi.org/10.48130/prkm-0026-0023

study examines acyl fluoride amidation in water, with particular focus on the origin of the unusual selectivity observed under aqueous carbonate-mediated conditions. Notably, K_2CO_3, which afforded only 4% yield in PFP-mediated amidation in MeCN[34], promotes highly selective *N*-functionalization of acyl fluorides in water in the present system. Compared with acyl chlorides, their greater compatibility with aqueous media removes a fundamental barrier to efficient acylation under aqueous conditions[35,36]. However, the exceptional reactivity and selectivity observed in water cannot be explained solely by the hydrolytic stability or electrophilic character of the acyl fluoride[37,38]. Instead, accumulating evidence suggests that reaction selectivity is governed by factors beyond the intrinsic properties of the acylating agent, particularly the inorganic cation and the surrounding aqueous solvation environment[36,39,40]. Despite their potential importance, the mechanistic roles of these factors in controlling acyl transfer and determining the balance between productive *N*-functionalization and competing hydrolysis remain largely unexplored.

Herein, we report a kinetic and mechanistic investigation of carbonate-mediated amidation of amines with acyl fluorides in water. By integrating reaction kinetics, spectroscopic characterization, control experiments, and density functional theory (DFT) calculations, we identify a water-solvated coordination environment resembling an 18-crown-6–K^+ complex, arising from the cooperative assembly of an acyl fluoride, a potassium ion, and water. This unique structural motif enables carbonate-driven acyl transfer and the formation of a hydrolytically stable carbonic mixed anhydride, thereby achieving highly selective *N*-functionalization under fully aqueous conditions. More broadly, this work uncovers a previously unrecognized mode of aqueous acyl transfer and identifies cooperative acyl fluoride–K^+–H_2O assembly as a key determinant of reaction pathway selection and chemoselectivity in water, establishing a viable mechanistic alternative to classical Schotten–Baumann chemistry (Fig. 1).

Materials and methods

Materials and chemicals

All commercially available reagents were used as received unless otherwise specified. Acyl chlorides used for the synthesis of the corresponding acyl fluorides, benzoyl fluoride (> 98.0%, GC), and amines (> 99.0%, GC) were purchased from Tokyo Chemical Industry Co., Ltd. (TCI). Anhydrous potassium fluoride (99%) was purchased from Thermo Scientific Chemicals, and anhydrous potassium carbonate (99.5%) was purchased from Daejung Chemicals & Metals Co., Ltd. Deionized water was used as the reaction solvent for all aqueous amidation reactions.

Experimental procedures

General procedure A for the synthesis of acyl fluorides 1

Potassium fluoride (1.0 mmol, 2.0 equiv.) was added to a stirred solution of the corresponding acyl chloride (0.5 mmol) in anhydrous acetone (2.5 mL, 0.2 M). The reaction mixture was stirred at room temperature for the specified time. After completion of the reaction, the resulting inorganic salts were removed by filtration, and the filtrate was purified according to the previously reported procedure to afford the corresponding acyl fluoride **1**.

General procedure B for the synthesis of amides 3

To a stirred solution of amine **2** (1.0 mmol) in deionized water (5 mL, 0.2 M) were added potassium carbonate (K_2CO_3, 1.2 mmol,

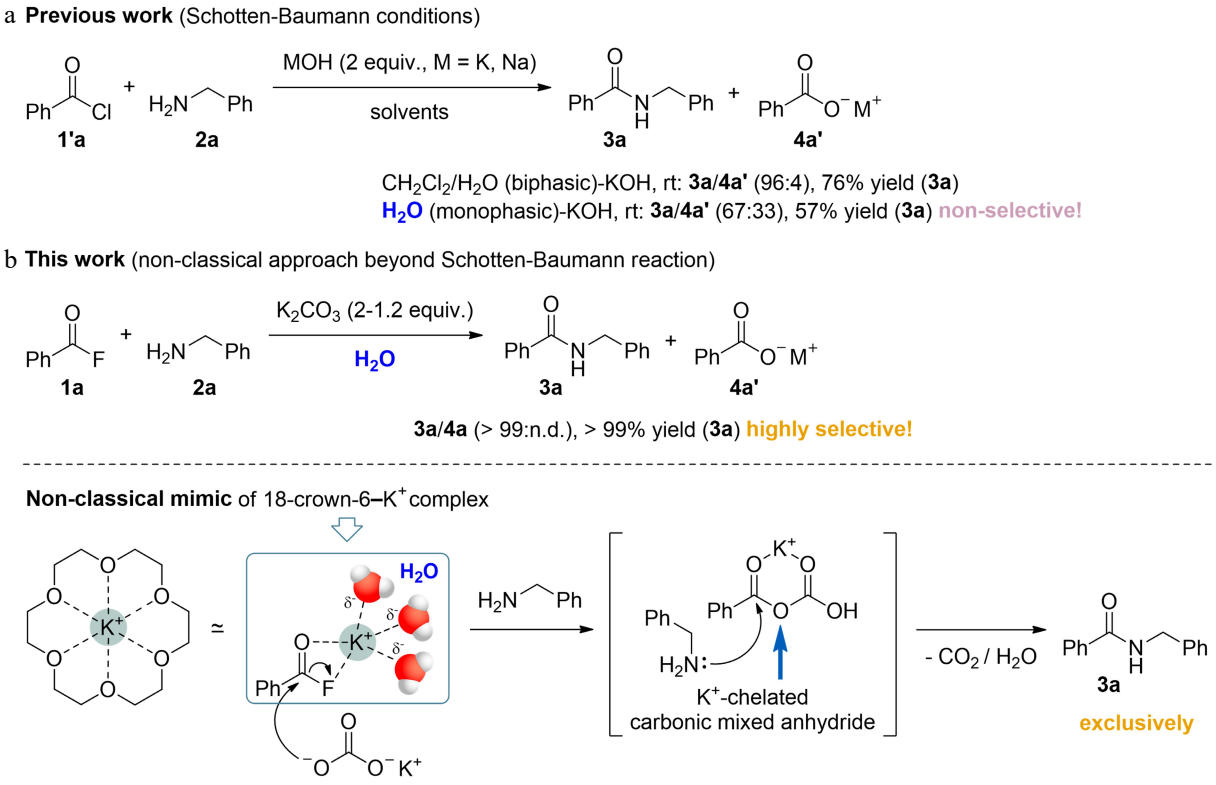


Fig. 1 (a) Classical Schotten–Baumann reaction employing a typical biphasic system (CH_2Cl_2/H_2O, KOH). (b) Beyond Schotten–Baumann chemistry: a non-classical 18-crown-6–K^+ mimic converts carbonate from a simple acid scavenger into a nucleophilic acyl-transfer partner, generating a hydrolytically stable carbonic mixed anhydride that redirects acyl-transfer reactivity toward productive *N*-functionalization while suppressing hydrolytic side reactions.

1.2 equiv.) and acyl fluoride **1** (1.0 mmol, 1.0 equiv.). The mixture was stirred at room temperature for 1 h. Upon completion of the reaction, the reaction mixture was acidified with 1 N HCl, resulting in precipitation of the corresponding amide. The resulting solid was isolated by vacuum filtration, washed thoroughly with water, and dried under reduced pressure to afford the corresponding amide **3**.

Results and discussion

To delineate the factors governing selective *N*-functionalization, the reaction of benzoyl fluoride **1a** with benzylamine **2a** was systematically investigated, with the corresponding benzoyl chloride **1'a** serving as a comparative reference, under a range of solvent and base conditions (Table 1). Under classical Schotten–Baumann conditions employing a biphasic CH_2Cl_2-H_2O or Et_2O-H_2O system, hydrolysis of benzoyl chloride **1'a** was effectively suppressed, with benzoic acid **4a** formed in less than 10% yield (particularly in the CH_2Cl_2–H_2O biphasic system, where the yield of **4a** was below 5%). Nevertheless, the desired amide **3a** was obtained in only moderate yields (61%–76%), presumably owing to the inherent limitations of biphasic operation, where productive acylation relies on interfacial mass transfer between the aqueous and organic phases (entries 1–2). To eliminate the use of environmentally hazardous halogenated solvents such as CH_2Cl_2 and highly flammable solvents such as Et_2O, the reaction was subsequently conducted in water as the sole reaction medium using benzylamine **2a** in the presence of 2.0 equivalents of KOH. Under these conditions, productive amidation was markedly diminished, affording **3a** in only moderate yield (57%) together with benzoic acid **4a** (19% yield), indicating that hydrolysis became the dominant competing pathway (entry 3). To our surprise, despite the superior hydrolytic stability of benzoyl fluoride relative to benzoyl chloride, the reaction exhibited a comparable level of hydrolysis, affording product distributions similar to those obtained with the corresponding acyl chloride (entry 4). Interestingly, the reaction outcome changed dramatically when hydroxide was replaced with potassium carbonate (K_2CO_3). Under identical conditions, benzoyl fluoride **1a** exhibited an abrupt enhancement in selectivity, furnishing amide **3a** in near-quantitative yield while completely suppressing the formation of benzoic acid **4a** (entry 6). In contrast, the corresponding acyl chloride remained susceptible to hydrolysis, revealing a fundamental difference in reactivity between the two acylating agents (entry 5). Notably, reducing the amount of K_2CO_3 from 2.0 to 1.2 equivalents afforded the optimal result, delivering amide **3a** in > 99% yield while completely eliminating the formation of the hydrolytic by-product **4a**, with the reaction reaching completion within 1 h. Under otherwise identical conditions, replacing K_2CO_3 with KOH markedly reduced both the yield of amide **3a** and the chemoselectivity of the reaction (entry 8). These results identify carbonate as an essential promoter of productive *N*-functionalization.

Having established the optimized conditions, the substrate scope of the aqueous *N*-functionalization protocol was investigated. Acyl fluorides bearing *para*-substituted aryl groups with either electron-withdrawing (–Br, –CN, $–NO_2$) or electron-donating (–OMe) substituents underwent smooth coupling with benzylamine, and high selectivity for *N*-functionalization was maintained irrespective of the electronic nature of the aryl substituents. Broad substrate compatibility was further demonstrated with structurally diverse amines, including simple primary amines and chiral primary amines, all of which furnished the desired amides in excellent yields. Notably, methylamine hydrochloride, a bench-stable surrogate for volatile methylamine, proved to be an equally competent coupling partner. Even when employed directly under the standard aqueous basic conditions, without prior liberation of the free amine, it afforded the corresponding amide **3f** in > 99% yield. The scope was further extended to acyclic secondary amines with different steric and electronic properties. Dimethylamine, diisopropylamine, diphenylamine, and dibenzylamine furnished the corresponding tertiary amides **3l–3o** in 98%–99% isolated yields. Notably, both sterically hindered diisopropylamine and the less nucleophilic diphenylamine underwent efficient amidation without appreciable competing hydrolysis, showing that increased steric demand and reduced amine nucleophilicity did not significantly compromise the selectivity of the aqueous carbonate-mediated reaction.

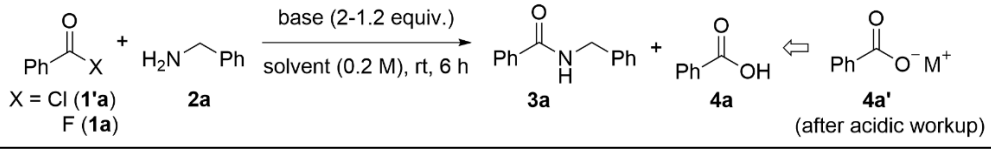
Overall, the protocol accommodated electronically differentiated acyl fluorides **1** and structurally diverse primary and secondary amines **2**, providing the corresponding amides **3** in generally high yields (Fig. 2).

Kinetic studies and control experiments

To evaluate this non-classical alternative to the Schotten–Baumann reaction, the reactivity of benzoyl fluoride **1a** under aqueous carbonate and hydroxide conditions was directly

Table 1. Optimization of reaction conditions[a].

Entry	Halide source	Base (equiv.)	Solvent	Ratio of **3a** : **4a**	Yield of **3a** (%)
1	Cl (**1'a**)	KOH (2.0)	CH_2Cl_2/H_2O (v/v = 1:1)	96:4	76
2	Cl (**1'a**)	KOH (2.0)	Et_2O/H_2O (v/v = 1:1)	90:10	61
3	Cl (**1'a**)	KOH (2.0)	H_2O	67:33	57
4	F (**1a**)	KOH (2.0)	H_2O	68:32	65
5[c]	Cl (**1'a**)	K_2CO_3 (2.0)	H_2O	80:20	72
6[c]	F (**1a**)	K_2CO_3 (2.0)	H_2O	> 99:n.d.	> 99[d]
7[c]	**F (1a)**	**K_2CO_3 (1.2)**	**H_2O**	**> 99:n.d.**	**> 99[d]**
8	F (**1a**)	KOH (1.2)	H_2O	84:16	83



[a] General conditions: benzoyl halide (**1a** or **1'a**, 1 mmol), base (1.2–2 equiv.), solvent (0.2 M), rt, 6 h. [b] Yields and product ratios were determined by ^{1}H NMR spectroscopy analysis using 1,3,5-trimethoxybenzene as an internal standard. [c] Reaction time: 1 h. [d] Isolated yield.

https://doi.org/10.48130/prkm-0026-0023

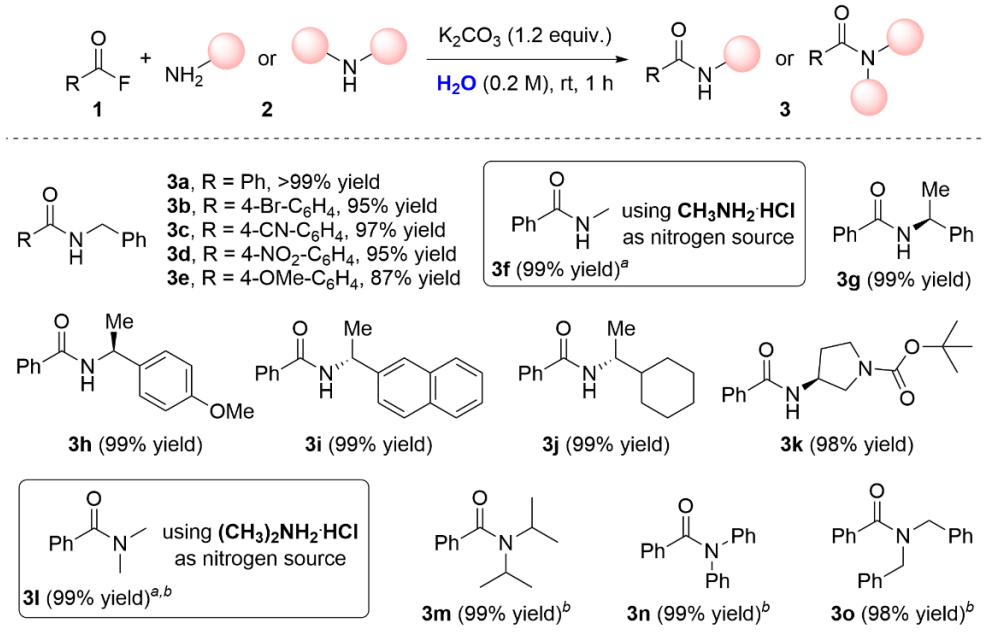


Fig. 2 Reaction scope and general conditions: acyl fluoride 1 (1 equiv.), amine 2 (1 mmol), K_2CO_3 (1.2 equiv.), H_2O (0.2 M, 5 mL), rt, 1 h. Yields refer to isolated yields. [a] Using 2.2 equiv. of K_2CO_3. [b] Reaction time is 6 h.

compared with that of the corresponding benzoyl chloride **1'a**. The initial screening studies revealed that benzoyl chloride **1'a** remained highly susceptible to hydrolysis under aqueous conditions, whereas benzoyl fluoride **1a** exhibited markedly higher chemoselectivity toward productive *N*-functionalization in the presence of K_2CO_3. To examine the kinetic basis of this difference, time-course experiments were performed for the reaction of benzoyl fluoride **1a** with benzylamine **2a** using K_2CO_3 or KOH under identical aqueous conditions (Fig. 3).

Under K_2CO_3-mediated conditions, rapid consumption of benzoyl fluoride **1a** was accompanied by near-quantitative formation of amide **3a** within 0.75–1 h, whereas benzoic acid **4a** remained undetectable throughout the reaction course. This result indicates that hydrolysis of the acyl fluoride is effectively suppressed, thereby favoring productive *N*-functionalization over the competing hydrolysis pathway. In sharp contrast, replacement of K_2CO_3 with KOH led to rapid formation of benzoic acid **4a**, which reached 15%–16% during the initial stage of the reaction and persisted throughout the reaction course. Although amide **3a** was formed concurrently, complete consumption of benzoyl fluoride **1a** required approximately 2 h, and the final yield of amide **3a** reached only 83%.

To quantitatively compare the reaction profiles, the early-time decay of benzoyl fluoride **1a** (0–15 min) was fitted to a single-exponential decay function, $[\mathbf{1a}]_t/[\mathbf{1a}]_0 = e^{-k_{app}t}$, where $[\mathbf{1a}]_t/[\mathbf{1a}]_0$ represents the normalized amount of benzoyl fluoride **1a** remaining at time *t*. Because the reactions were not conducted under strict pseudo-first-order conditions, the fitted values are reported as apparent decay constants (k_{app}) rather than elementary rate

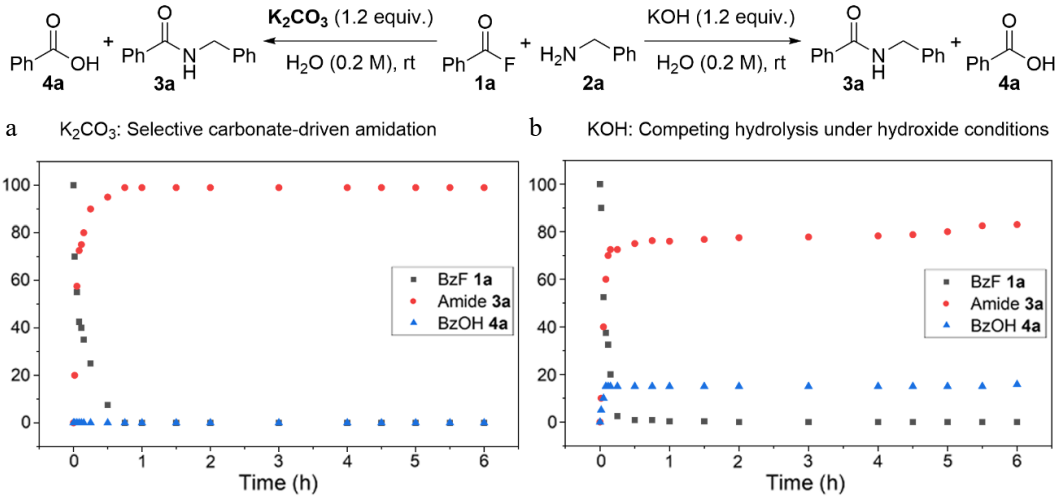


Fig. 3 Time-course profiles for the aqueous amidation of benzoyl fluoride 1a with benzylamine 2a using (a) K_2CO_3 or (b) KOH. The K_2CO_3-mediated reaction rapidly affords amide 3a in near-quantitative yield within 0.75–1 h without detectable formation of benzoic acid 4a, whereas the KOH-mediated reaction is accompanied by competing hydrolysis, leading to the accumulation of benzoic acid 4a and requiring approximately 2 h for complete conversion.

constants. The fitting gave k_{app} = 0.229 min^{-1} for the K_2CO_3-mediated reaction and k_{app} = 0.241 min^{-1} for the KOH-mediated reaction, corresponding to apparent half-lives ($t_{1/2}$) of 3.03 and 2.88 min, respectively. The similar k_{app} values indicate that the early-time rates of benzoyl fluoride consumption are comparable under the two conditions. The corresponding experimental data, nonlinear regression fits, and fitted kinetic parameters are provided in Supplmentary File 1 (Tables S1, S2, and Fig. S1). In contrast, the product formation profiles differ markedly: at 15 min, the K_2CO_3-mediated reaction afforded 90% amide **3a** with no detectable **4a**, whereas the KOH-mediated reaction afforded 72.5% **3a** together with 15% **4a**. Thus, the major kinetic difference between the two systems lies in the partitioning of consumed acyl fluoride between productive amidation and competing hydrolysis rather than in the rate of substrate disappearance.

These results show that the exceptional chemoselectivity under K_2CO_3-mediated aqueous conditions does not arise from accelerated consumption of benzoyl fluoride. Instead, substrate consumption is directed predominantly toward productive *N*-functionalization with minimal competing hydrolysis. This behavior differs markedly from the KOH-mediated reaction, in which amidation and hydrolysis occur concurrently. Unlike the classical Schotten–Baumann reaction, in which hydroxide promotes competing hydrolysis of the acyl halide, this distinct reaction-pathway partitioning supports the involvement of a non-classical carbonate-mediated acyl-transfer process. As discussed below, spectroscopic and computational studies further support the involvement of a carbonic mixed anhydride as the key intermediate in this pathway.

The striking reversal in reactivity observed under carbonate-mediated aqueous conditions cannot be rationalized solely by the intrinsic leaving-group ability of the acyl halide (Fig. 4). Under classical Schotten–Baumann conditions, acyl chlorides and acyl fluorides exhibited comparable amidation efficiencies together with similar levels of hydrolytic by-product formation, despite the substantially stronger C–F bond of acyl fluorides, as reflected by the markedly higher bond dissociation energy (BDE) of the C–F bond (121.6 kcal·mol^{-1}) relative to the corresponding C–Cl bond in acyl chlorides (83.8 kcal·mol^{-1}). These results indicate that hydroxide-mediated acyl transfer and hydrolysis dominate the reaction outcome irrespective of the intrinsic leaving-group properties of the acyl halide (see Table 1, entries 3–4).

In sharp contrast, this reactivity trend was completely reversed in the presence of K_2CO_3. Although acyl fluorides are intrinsically less reactive acylating agents than acyl chlorides, they exhibited exceptional *N*-functionalization efficiency under aqueous carbonate-mediated conditions. To experimentally examine the role of the alkali-metal countercation, Li_2CO_3, Na_2CO_3, K_2CO_3, and Cs_2CO_3 were evaluated under otherwise identical conditions, with carbonate maintained as the common anion (Supplmentary File 1: Table S3). Li_2CO_3 afforded amide **3a** in 91% yield with a **3a : 4a** ratio of 97:3, whereas Na_2CO_3 and K_2CO_3 afforded **3a** in 96% and > 99% yield, respectively, with no detectable hydrolysis. In contrast, Cs_2CO_3 afforded **3a** in 71% yield with a **3a : 4a** ratio of 96:4. This countercation dependence shows that the identity of the alkali-metal cation influences the efficiency and selectivity of the carbonate-mediated acyl-transfer process, providing experimental support for cation participation in the reaction.

Consistent with the experimentally observed countercation effect and previous reports of alkali-metal coordination to anhydride-type species[41], the unusual reactivity arises from the cooperative organization of an acyl fluoride, a potassium ion (derived from K_2CO_3), and water, which activates the acyl fluoride toward nucleophilic attack by carbonate despite the intrinsically lower nucleophilicity of carbonate relative to hydroxide. Consequently, carbonate functions as a nucleophilic acyl-transfer partner to generate a carbonic mixed anhydride (**A**). DFT calculations further suggest that the carbonic mixed anhydride can associate with K$^+$ in a water-solvated coordination environment, providing a structural model consistent with the experimentally observed cation effect. To experimentally verify the formation of this transient intermediate, *in situ* ^{1}H NMR

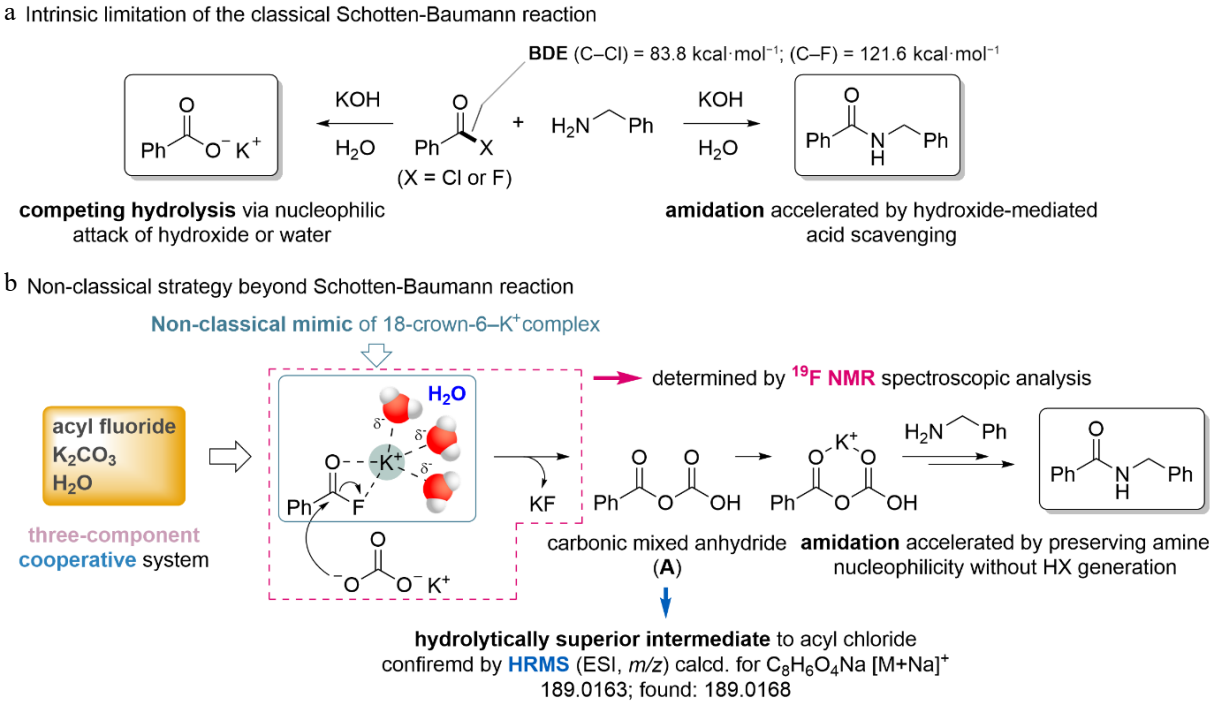


Fig. 4 Mechanistic distinction between the classical Schotten–Baumann reaction and the carbonate-mediated non-classical acyl-transfer pathway.

https://doi.org/10.48130/prkm-0026-0023

spectroscopy was employed (Fig. 5). Owing to its high reactivity and rapid decomposition during workup, the carbonic mixed anhydride was monitored directly using aliquots withdrawn from the reaction mixture.

The appearance of the characteristic ^{1}H NMR signals of the carbonic mixed anhydride, accompanied by the simultaneous disappearance of the acyl fluoride signals, provides direct experimental evidence for its transient formation under the reaction conditions. The formation of this intermediate was further supported by high-resolution mass spectrometry (HRMS), which showed an ion at *m/z* 189.0168 corresponding to $[M + Na]^+$ (calcd for $C_8H_6O_4Na$ $[M + Na]^+$: 189.0163).

In addition, carbonate-mediated C–F bond cleavage was directly monitored by ^{19}F NMR spectroscopy, which revealed concomitant consumption of the acyl fluoride and formation of KF during the reaction (Fig. 6). These observations provide direct experimental evidence that carbonate participates as a nucleophile in the initial acyl-transfer step. DFT calculations further provide a molecular-level rationale for the proposed activation mode and the subsequent carbonate-mediated acyl-transfer pathway (Fig. 7). The resulting carbonic mixed anhydride exhibits enhanced hydrolytic stability relative to the corresponding acyl halide, thereby favoring productive *N*-functionalization over competing hydrolysis. Furthermore, because the carbonate-mediated acyl-transfer pathway proceeds without the generation of HX (e.g., HCl or HF), amine nucleophilicity is preserved throughout the reaction, enabling near-quantitative amidation under fully aqueous conditions.

NMR spectroscopic analysis

For both ^{1}H and ^{19}F NMR spectroscopic analyses, aliquots were withdrawn directly from the reaction mixture, immediately dissolved in CD_3OD containing 2-chloro-4-fluorotoluene as an internal standard (IS), and analyzed without workup or purification.

In situ observation of carbonic mixed anhydride formation by ^{1}H NMR spectroscopy

The appearance of characteristic ^{1}H NMR signals attributable to the carbonic mixed anhydride, accompanied by the simultaneous disappearance of the corresponding acyl fluoride signals, confirms its *in situ* formation under the reaction conditions (Fig. 5).

Direct observation of carbonate-mediated C–F bond cleavage and KF formation by ^{19}F NMR spectroscopy

Progressive disappearance of the acyl fluoride resonance at δ 15.5 ppm was accompanied by the simultaneous emergence of a new signal at δ −165.9 ppm, which matched that of an authentic KF (**B**) reference (Fig. 6). These correlated spectral changes provide direct experimental evidence that carbonate attacks the activated acyl fluoride to initiate C–F bond cleavage, leading to KF formation and revealing its previously unrecognized role as the nucleophile responsible for the initial acyl-transfer event.

Computational modelling

All density functional theory (DFT) calculations were performed using the ORCA 6.1.1 program package[42]. Geometry optimizations and transition-state searches were carried out using the B3LYP functional in conjunction with Grimme's D3BJ dispersion correction and the def2-SVP basis set[43]. Solvation effects were incorporated using the conductor-like polarizable continuum model (CPCM) with water as the implicit solvent[44]. Harmonic vibrational frequency

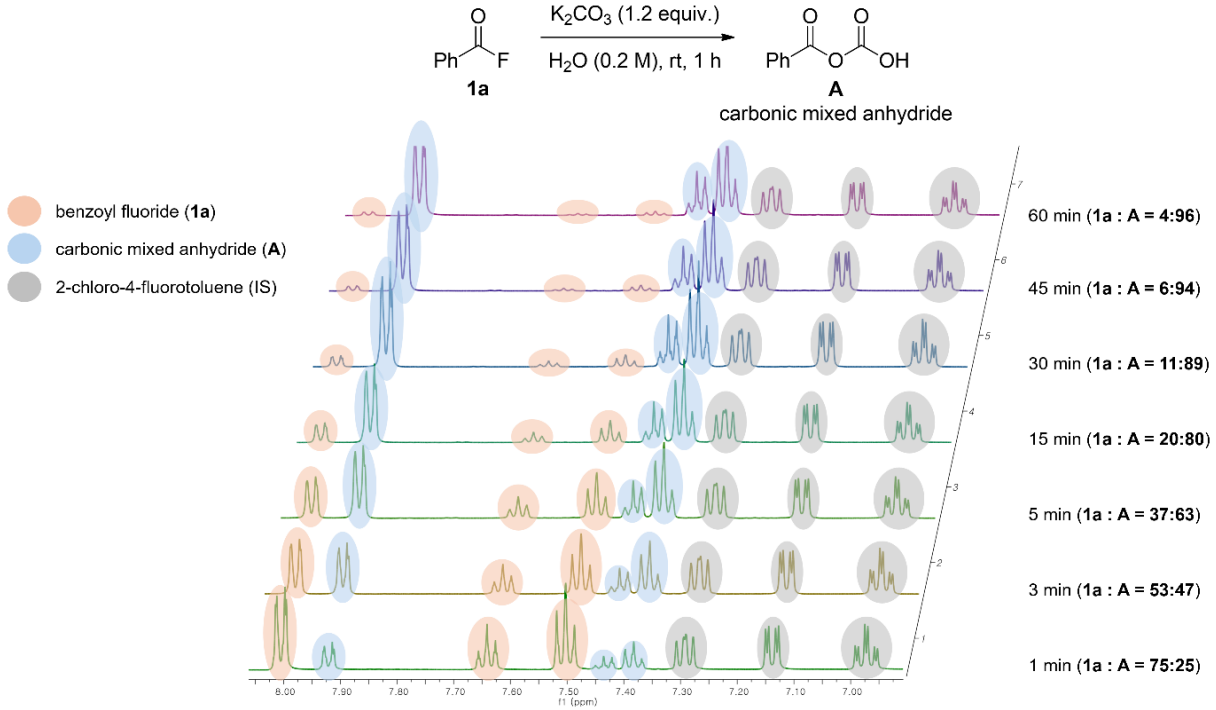


Fig. 5 ^{1}H NMR spectroscopic evidence for the formation of the carbonic mixed anhydride intermediate during the carbonate-mediated acyl-transfer reaction.

https://doi.org/10.48130/prkm-0026-0023

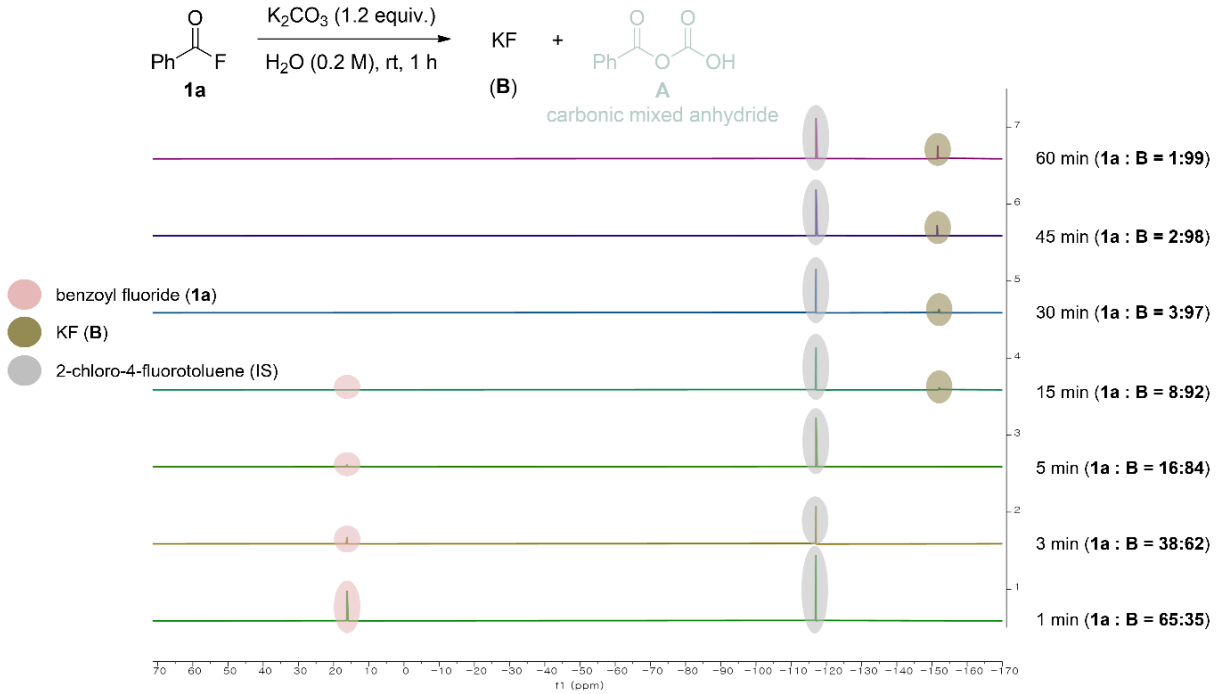


Fig. 6 ^{19}F NMR spectroscopic evidence for carbonate-mediated C–F bond cleavage through the concomitant consumption of acyl fluoride and formation of KF during the reaction.

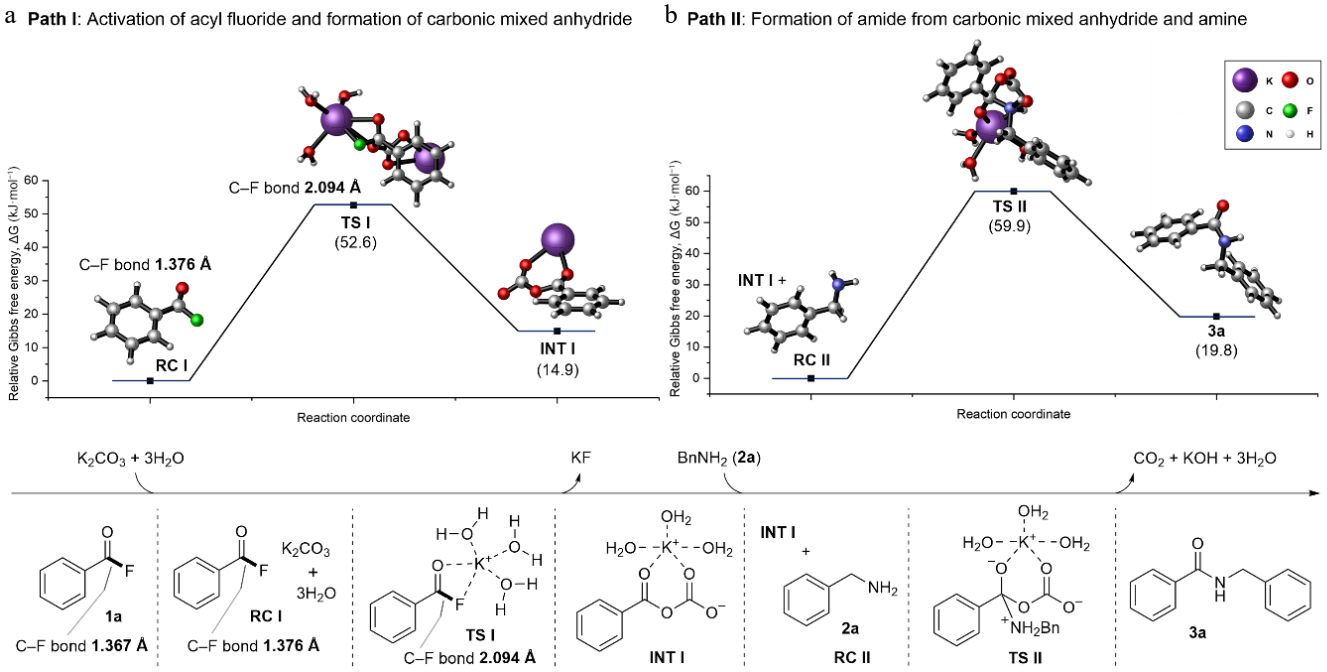


Fig. 7 DFT-calculated Gibbs free-energy profiles and representative optimized structures for the carbonate-mediated amidation of benzoyl fluoride. (a) Path I: carbonate-mediated activation of benzoyl fluoride within the non-classical 18-crown-6–K^+ mimic incorporating three explicit water molecules, leading to C–F bond cleavage and formation of the K^+–associated carbonic mixed anhydride. (b) Path II: amide formation via nucleophilic acyl substitution of the K^+–associated carbonic mixed anhydride by benzylamine.

calculations were performed at the same level of theory to verify the nature of the stationary points and to obtain Gibbs free energy corrections[45].

All local minima were confirmed by the absence of imaginary frequencies, whereas each transition state was characterized by a single imaginary frequency corresponding to the reaction coordinate. The carbonate-mediated activation step and the subsequent amine-addition step were modeled separately to avoid artificial distortions in the calculated energy profile arising from the spectator amine, KF, and water-cluster rearrangements. Three explicit water molecules were incorporated into the carbonate- and potassium-associated structures to represent the local aqueous coordination environment. Relative Gibbs free energies were obtained at the B3LYP-D3BJ/def2-SVP/CPCM (water) level and are

https://doi.org/10.48130/prkm-0026-0023

reported in kJ·mol^{-1} relative to the corresponding reactant complex within each mechanistic section. The calculated energy profiles are used to compare relative energetic trends and structural features along the proposed reaction pathway rather than represent method-independent absolute activation barriers. Molecular structures were visualized using CYLview[46].

To gain mechanistic insight into the carbonate-mediated amidation of acyl fluorides, the reaction pathway was divided into two mechanistic stages for DFT analysis. **Path I** describes the carbonate-mediated activation of benzoyl fluoride through the formation of the non-classical 18-crown-6–K^+ mimic incorporating three explicit water molecules, culminating in C–F bond cleavage and the generation of a K^+–chelated carbonic mixed anhydride. **Path II** describes the subsequent nucleophilic attack of benzylamine on the K^+–chelated carbonic mixed anhydride, leading to the amide product accompanied by the release of CO_2, KOH, and H_2O. This separate treatment allows the energetics of each elementary process to be evaluated relative to its own reactant complex, thereby avoiding artificial energy distortions arising from spectator species and cluster rearrangements. The resulting Gibbs free-energy profiles together with representative optimized structures are summarized in Fig. 7.

The DFT calculations reveal that carbonate-mediated activation of benzoyl fluoride within the non-classical 18-crown-6–K^+ mimic proceeds via **TS I** to generate the K^+-associated carbonic mixed anhydride, which serves as the key intermediate in the proposed carbonate-driven acyl-transfer pathway (Fig. 7a). **TS I** is located 52.6 kJ·mol^{-1} above the reactant complex, corresponding to the activation barrier for carbonate-mediated C–F bond cleavage. Structural analysis of the optimized geometries along the reaction coordinate provides further insight into the activation process. In the reactant complex (**RC I**), the calculated C–F bond length of benzoyl fluoride is 1.376 Å, essentially identical to that of free benzoyl fluoride (1.367 Å), indicating that little or no C–F bond activation occurs prior to carbonate attack. At **TS I**, however, the C–F bond is substantially elongated to 2.094 Å. This marked elongation reflects significant activation of the acyl fluoride within the cooperative acyl fluoride–K^+–H_2O assembly of the non-classical 18-crown-6–K^+ mimic, accompanied by increased electrophilicity of the carbonyl carbon. Consequently, despite the resonance-stabilized and inherently weak nucleophilic character of carbonate, the activated acyl fluoride undergoes efficient carbonate-mediated acyl transfer to generate the K^+–associated carbonic mixed anhydride. These results provide computational evidence that the non-classical assembly enables a distinct carbonate-driven acyl-transfer pathway through concerted C–F bond activation and carbonyl polarization.

The subsequent amide-forming step was investigated in **Path II** (Fig. 7b), where the K^+-associated carbonic mixed anhydride generated in **Path I** serves as the electrophilic acyl-transfer intermediate. In the reactant complex (**RC II**), benzylamine is positioned in close proximity to the acyl carbon of **INT I**, providing a preorganized geometry for nucleophilic attack. **TS II** is located 59.9 kJ·mol^{-1} above **RC II** and corresponds to the C–N bond-forming transition state. The relatively high free-energy barrier reflects the energetic demand associated with the tetrahedral transition-state geometry required for nucleophilic acyl substitution. Following passage through **TS II**, the reaction proceeds directly to the desired amide product **3a** with concomitant release of CO_2, KOH, and H_2O. The product state lies 19.8 kJ·mol^{-1} above **RC II** but 40.1 kJ·mol^{-1} below **TS II**, demonstrating that the reaction proceeds downhill in free energy after crossing the C–N bond-forming transition state. Together with the **Path I** calculations, these results support a stepwise carbonate-driven amidation mechanism in which potassium carbonate first converts the acyl fluoride into a K^+–associated carbonic mixed anhydride, which subsequently undergoes nucleophilic acyl substitution by benzylamine **2a** to furnish the amide product **3a**.

Conclusions

In summary, we have developed a sustainable aqueous amidation protocol based on carbonate-mediated acyl transfer of acyl fluorides and elucidated its kinetic and mechanistic origin through reaction kinetics, NMR spectroscopy, control experiments, HRMS, and DFT calculations. Rather than proceeding through the conventional hydroxide-mediated pathway characteristic of the classical Schotten–Baumann reaction, the transformation operates through a non-classical acyl-transfer mechanism initiated by the cooperative organization of an acyl fluoride, a potassium ion (derived from K_2CO_3), and water. This unique activation mode enables carbonate to participate directly in acyl transfer, leading to the formation of a hydrolytically stable carbonic mixed anhydride while avoiding HX generation. The combination of enhanced resistance toward hydrolysis and preservation of amine nucleophilicity enables productive *N*-functionalization to consistently outcompete competing hydrolysis under fully aqueous conditions. Beyond providing a molecular-level rationale for the unusual reactivity of acyl fluorides in water, this work establishes a mechanistic foundation for the rational design of selective aqueous acyl-transfer chemistry and expands the conceptual boundaries of classical Schotten–Baumann methodology. Ongoing studies in our laboratory are directed toward applying this non-classical acyl-transfer strategy to a broader range of bond-forming reactions and sustainable synthetic transformations in aqueous media.

Author contributions

The authors confirm their contributions to the paper as follows: experiments, data analysis, writing – original draft: Kim GH; manuscript review and editing, conceptualization, project supervision, funding acquisition: Yang JW. All authors reviewed the results and approved the final version of the manuscript.

Data availability

All data generated or analyzed during this study are included in this published article and its supplementary information files.

Acknowledgments

This work was supported by the National Research Foundation of Korea (NRF) grant funded by the Korean government (MSIT) (RS-2026-25478335 and RS-2023-00219859). Additionally, the generous support of the Korea Basic Science Institute (National Research Facilities and Equipment Center) grant, funded by the Ministry of Education (RS-2022-NF000854), is gratefully acknowledged.

Conflict of interest

The authors declare that they have no conflict of interest.

Supplementary information accompanies this paper online at: https://doi.org/10.48130/prkm-0026-0023.

Dates

Received 15 July 2026; Revised 26 August 2026; Accepted 9 September 2026; Published online 3 November 2026

References

[1] Blackmond DG. 2015. Kinetic profiling of catalytic organic reactions as a mechanistic tool. *Journal of the American Chemical Society* 137:10852–10866

[2] Jorner K, Tomberg A, Bauer C, Sköld C, Norrby PO. 2021. Organic reactivity from mechanism to machine learning. *Nature Reviews Chemistry* 5:240–255

[3] Plonka A. 2000. Recent developments in dispersive kinetics. *Progress in Reaction Kinetics and Mechanism* 25:109–217

[4] Yu JS, Liu YL, Tang J, Wang X, Zhou J. 2014. Highly efficient "on water" catalyst-free nucleophilic addition reactions using difluoroenoxysilanes: dramatic fluorine effects. *Angewandte Chemie (International Ed in English)* 53:9512–9516

[5] Canavelli P, Islam S, Powner MW. 2019. Peptide ligation by chemoselective aminonitrile coupling in water. *Nature* 571:546–549

[6] Kariyawasam LS, Hartley CS. 2017. Dissipative assembly of aqueous carboxylic acid anhydrides fueled by carbodiimides. *Journal of the American Chemical Society* 139:11949–11955

[7] Scattolin T, Bouayad-Gervais S, Schoenebeck F. 2019. Straightforward access to *N*-trifluoromethyl amides, carbamates, thiocarbamates and ureas. *Nature* 573:102–107

[8] Sabatini MT, Boulton LT, Sheppard TD. 2017. Borate esters: simple catalysts for the sustainable synthesis of complex amides. *Science Advances* 3:e1701028

[9] Boström J, Brown DG, Young RJ, Keserü GM. 2018. Expanding the medicinal chemistry synthetic toolbox. *Nature Reviews Drug Discovery* 17:709–727

[10] De Berardinis L, Vitali D, Cerea P, Bertolini G, Cabri W, et al. 2024. Rediscovery of an old named reaction: from micellar catalysis to unusual Schotten–Baumann conditions. *Organic Process Research & Development* 28:3578–3586

[11] Santos AS, Silva AMS, Marques MMB. 2020. Sustainable amidation reactions–recent advances. *European Journal of Organic Chemistry* 2020:2501–2516

[12] King JF, Rathore R, Lam JYL, Guo ZR, Klassen DF. 1992. pH optimization of nucleophilic reactions in water. *Journal of the American Chemical Society* 114:3028–3033

[13] Montalbetti CAGN, Falque V. 2005. Amide bond formation and peptide coupling. *Tetrahedron* 61:10827–10852

[14] El-Faham A, Albericio F. 2011. Peptide coupling reagents, more than a letter soup. *Chemical Reviews* 111:6557–6602

[15] Nakatsuji H, Morita JI, Misaki T, Tanabe Y. 2006. Water solvent method for esterification and amide formation between acid chlorides and alcohols promoted by combined catalytic amines: synergy between *N*-methylimidazole and *N,N,N′,N′*-tetramethylethylenediamine (TMEDA). *Advanced Synthesis & Catalysis* 348:2057–2062

[16] Bentley TW, Llewellyn G, McAlister JA. 1996. S_N2 mechanism for alcoholysis, aminolysis, and hydrolysis of acetyl chloride. *The Journal of Organic Chemistry* 61:7927–7932

[17] Bunton CA, Gillitt ND, Mhala MM, Moffatt JR, Yatsimirsky AK. 2000. Micellar charge effects upon hydrolyses of substituted benzoyl chlorides. Their relation to mechanism. *Langmuir* 16:8595–8603

[18] Magosso M, van den Berg M, van der Schaaf J. 2021. Kinetic study and modeling of the Schotten–Baumann synthesis of peroxyesters using phase-transfer catalysts in a capillary microreactor. *Reaction Chemistry & Engineering* 6:1574–1590

[19] Polster CS, Cole KP, Burcham CL, Campbell BM, Frederick AL, et al. 2014. Pilot-scale continuous production of LY2886721: amide formation and reactive crystallization. *Organic Process Research & Development* 18:1295–1309

[20] Jordan A, Stoy P, Sneddon HF. 2021. Chlorinated solvents: their advantages, disadvantages, and alternatives in organic and medicinal chemistry. *Chemical Reviews* 121:1582–1622

[21] Jordan A, Hall CGJ, Thorp LR, Sneddon HF. 2022. Replacement of less-preferred dipolar aprotic and ethereal solvents in synthetic organic chemistry with more sustainable alternatives. *Chemical Reviews* 122:6749–6794

[22] Shi M, Ye N, Chen W, Wang H, Cheung C, et al. 2020. Simple synthesis of amides *via* their acid chlorides in aqueous TPGS-750-M. *Organic Process Research & Development* 24:1543–1548

[23] Hazra S, Gallou F, Handa S. 2022. Water: an underestimated solvent for amide bond-forming reactions. *ACS Sustainable Chemistry & Engineering* 10:5299–5306

[24] Zucchi A, Mattiello S, Maschio R, Bellotti V, Giovenzana GB, et al. 2024. Enabling amidation in water: micellar catalysis approach for sustainable synthesis of iopamidol. *RSC Advances* 14:39902–39907

[25] Okuda Y, Xu J, Ishida T, Wang CA, Nishihara Y. 2018. Nickel-catalyzed decarbonylative alkylation of aroyl fluorides assisted by Lewis-Acidic organoboranes. *ACS Omega* 3:13129–13140

[26] Ogiwara Y, Sakai N. 2020. Acyl fluorides in late-transition-metal catalysis. *Angewandte Chemie International Edition* 59:574–594

[27] Jung Y, Lee Y, Shin K. 2024. Catalytic synthesis of carbonyl compounds using acyl fluorides, carbamoyl fluorides, and fluoroformates: an overview. *Asian Journal of Organic Chemistry* 13:e202300661

[28] Hagmann WK. 2008. The many roles for fluorine in medicinal chemistry. *Journal of Medicinal Chemistry* 51:4359–4369

[29] Wang J, Sánchez-Roselló M, Aceña JL, del Pozo C, Sorochinsky AE, et al. 2014. Fluorine in pharmaceutical industry: fluorine-containing drugs introduced to the market in the last decade (2001–2011). *Chemical Reviews* 114:2432–2506

[30] Gillis EP, Eastman KJ, Hill MD, Donnelly DJ, Meanwell NA. 2015. Applications of fluorine in medicinal chemistry. *Journal of Medicinal Chemistry* 58:8315–8359

[31] Blanchard N, Bizet V. 2019. Acid fluorides in transition-metal catalysis: a good balance between stability and reactivity. *Angewandte Chemie International Edition* 58:6814–6817

[32] Bonnefoy C, Gallego A, Delobel C, Raynal B, Decourt M, et al. 2024. Unlocking the power of acyl fluorides: a comprehensive guide to synthesis and properties. *European Journal of Organic Chemistry* 27:e202400142

[33] Smedley CJ, Barrow AS, Spiteri C, Giel MC, Sharma P, et al. 2017. Sulfur-fluoride exchange (SuFEx)-mediated synthesis of sterically hindered and electron-deficient secondary and tertiary amides *via* acyl fluoride intermediates. *Chemistry – A European Journal* 23:9990–9995

[34] Brittain WDG, Cobb SL. 2021. Carboxylic acid deoxyfluorination and one-pot amide bond formation using pentafluoropyridine (PFP). *Organic Letters* 23:5793–5798

[35] Song BD, Jencks WP. 1989. Aminolysis of benzoyl fluorides in water. *Journal of the American Chemical Society* 111:8479–8484

[36] Kim GH, Kim DH, Lee Y, Yang JW. 2025. Sustainable synthesis of acyl fluoride *via* 1,3-chelation-assisted transhalogenation and its application in the valorization of biomass-derived alcohol in aqueous system. *Advanced Synthesis & Catalysis* 367:e202500103

[37] Serrano-Luginbühl S, Ruiz-Mirazo K, Ostaszewski R, Gallou F, Walde P. 2018. Soft and dispersed interface-rich aqueous systems that promote and guide chemical reactions. *Nature Reviews Chemistry* 2:306–327

[38] Narayan S, Muldoon J, Finn MG, Fokin VV, Kolb HC, et al. 2005. "On water": unique reactivity of organic compounds in aqueous suspension. *Angewandte Chemie (International Ed in English)* 44:3275–3279

[39] Xu P, Wang X, Wang T, Cao ZY, Yu JS, et al. 2025. The influence of C-F…H-X hydrogen-bonding interactions on the reactivity and selectivity of organic reactions. *Chemical Society Reviews* 54:9921–9938

[40] Kim GH, Lee Y, Shin K, Yang JW. 2026. Preorganization-driven site-selective *N*-functionalization of dual nucleophilic amino alcohols in basic aqueous media. *Organic Chemistry Frontiers* 13(17):5568–5577

https://doi.org/10.48130/prkm-0026-0023

[41] Spahr D, Bayarjargal L, Bykov M, Brüning L, Reuter TH, et al. 2023. High-pressure synthesis of acentric sodium pyrocarbonate, $Na_2[C_2O_5]$. *Dalton Transactions* 53:40–44

[42] Neese F. 2025. Software update: the *ORCA* program system—version 6.0. *WIREs Computational Molecular Science* 15:e70019

[43] Grimme S, Ehrlich S, Goerigk L. 2011. Effect of the damping function in dispersion corrected density functional theory. *Journal of Computational Chemistry* 32:1456–1465

[44] Weigend F, Ahlrichs R. 2005. Balanced basis sets of split valence, triple *Zeta* valence and quadruple *Zeta* valence quality for H to Rn: design and assessment of accuracy. *Physical Chemistry Chemical Physics* 7:3297–3305

[45] Garcia-Ratés M, Neese F. 2019. Efficient implementation of the analytical second derivatives of hartree-fock and hybrid DFT energies within the framework of the conductor-like polarizable continuum model. *Journal of Computational Chemistry* 40:1816–1828

[46] Legault CY. 2009. CYLview, 1.0b. Sherbrooke, QC, Canada: Université de Sherbrooke. www.cylview.org

Copyright: © 2026 by the author(s). Published by Maximum Academic Press, Fayetteville, GA. This article is an open access article distributed under Creative Commons Attribution License (CC BY 4.0), visit https://creativecommons.org/licenses/by/4.0/.